The International Supercritical CO_2 Energy Technologies Symposium
March 2 - 5, 2026, Pittsburgh, PA
Paper# 068

Heat Transfer Effects in Dense Gas Cylinder Flows

Anjini Chandra
Ph.D. Candidate
Stanford University
Stanford, CA

Hang Song
Postdoctoral Fellow, Center for Turbulence Research
Stanford University
Stanford, CA

Sanjiva K. Lele
Professor of Mechanical Engineering and Aeronautics and Astronautics
Stanford University
Stanford, CA

ABSTRACT

Supercritical carbon dioxide (sCO_2) plays an important role in the development of more efficient and sustainable power cycles. However, many components of sCO_2 cycles have yet to be optimized. Fundamental studies of external sCO_2 flows, such as those found over compressor and turbine blades, play an important role in understanding heat transfer within and optimizing the cycles. One canonical external configuration that can be extended to capture flow over turbomachinery blades is flow over a cylinder. This study characterizes heat transfer effects in ideal and dense gas cylinder flows using a set of large-eddy simulations (LES) that utilize the Peng-Robinson equation of state and related transport models.

INTRODUCTION

Supercritical carbon dioxide (sCO2) shows great promise in improving the efficiency and sustainability of power cycles [1, 2]. In sCO2 power plants, external flows, such as flow over turbine and compressor blades and heat exchanger components, play a crucial role in heat transfer and the overall efficiency of the cycle [3]. For instance, the boundary layers that form on the blades of turbomachinery affect heat fluxes into and out of the blades and could significantly decrease the efficiency of the cycle if they separate. In addition, external flows in heat exchangers ensure that the fluid is cooled sufficiently before it is compressed. However, heat transfer in external sCO2 flows is still under investigation; there is a need for high-fidelity and high-resolution simulations to provide a database that will inform the development of lower cost large-eddy simulation (LES) models to accurately predict the effects of such flows on cycle efficiency.

One external sCO2 flow of interest is compressible, turbulent flow over a cylinder. This flow represents a canonical configuration that can be extended to external flows such as flow over

an airfoil with a geometry representing a compressor or turbine blade. Recent studies have investigated wake phenomena in sCO2 flow over a cylinder. For example, Xie & Xie investigate vortex shedding and wake instabilities in low-Reynolds number cylinder flow [4]. The same authors study wake transition in sCO2 flows with slightly higher Reynolds number. Many other studies have focused on internal sCO2 flows such as those found in cylindrical channels [5-8]. However, these studies appear focused on low Reynolds numbers for external cylinder flows and otherwise on internal sCO2 flows with heat transfer. Very few studies have investigated compressible, sCO2 flow over a cylinder at Reynolds numbers above 3000 and with heat transfer and dense gas effects. The present study thus not only provides a foundation for future studies of sCO2 flow over an airfoil but also contributes to a high-resolution dataset of a sparsely-studied sCO2 flow configuration along with analysis of dense-gas heat transfer effects to the literature.

The goal of this study is to characterize heat transfer effects in compressible, turbulent dense-gas carbon-dioxide flow over a cylinder. Two wall-resolved LES of turbulent, sCO2 flow over a heated cylinder are run using PadeLibs, an in-house, GPU-accelerated solver [9], and compared to an analogous case with turbulent, calorically-perfect gas flow over a cylinder. Classical wall and wake statistics for cylinder flows are computed in addition to heat transfer statistics and related energy spectra. The simulation setup is described in section “Simulation Setup,” and the results are detailed in the section “Preliminary Results and Discussion.”

SIMULATION SETUP

This study investigates two cylinder flows under dense and ideal gas thermodynamic conditions. The thermodynamic parameters, freestream Reynolds number, freestream Mach number, wall-to-freestream density ratio, and other quantities are detailed in Table 1. Here, all quantities are normalized by the temperature and pressure at the critical point for carbon dioxide. The Reynolds number was chosen to be 3900 for a more direct comparison to canonical cylinder cases in the literature, and the freestream Mach number was chosen to be 0.2 to rule out large compressibility effects in the analysis of heat transfer.

	Wall temperature	**Freestream temperature**	**Freestream Reynolds number**	**Freestream Mach number**	**Density ratio**
Dense gas	0.95	1.15	3900	0.2	1.57
Perfect gas	0.95	1.50	3900	0.2	1.57

Table 1. Simulation thermodynamic parameters for dense and ideal gas cylinder flows.

The simulations in this study use a configuration very similar to that described in [10]. The computational mesh is an O-type mesh with radially- and azimuthally-varying mesh spacing to concentrate the mesh near the cylinder wall and in the wake region as shown in Figure 1. The radial mesh spacing function differs from the one in [10] to more isotropically distribute the mesh points in the wake region, but the azimuthal mesh spacing function is the same. Figure 2 shows the radial and azimuthal mesh coordinates as a function of normalized mesh index. The mesh resolutions for the perfect and dense gas cylinder cases are 384 x 320 x 128 and 384 x 256 x 128 grid points respectively where the three numbers represent resolution in the radial,

azimuthal, and spanwise directions respectively.

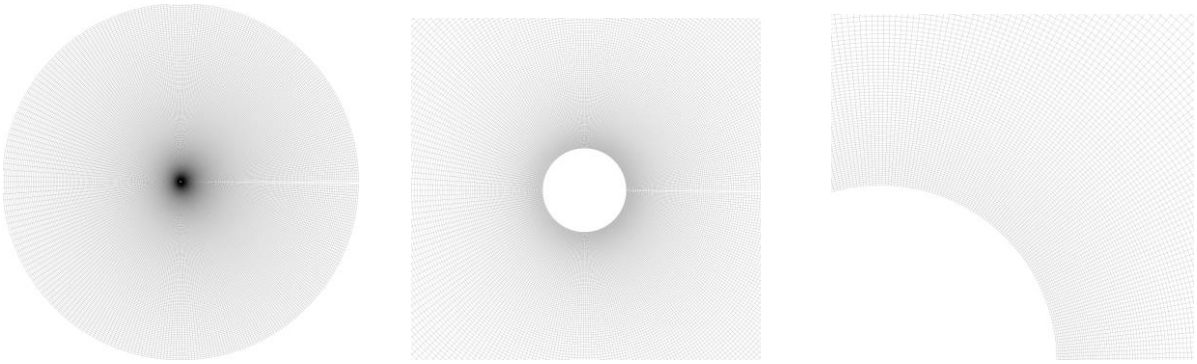

Figure 1. Computational mesh for dense gas cylinder case in the far field (left), near field (middle), and close to the cylinder wall (right). The mesh has an outer radius of 100 cylinder diameters.

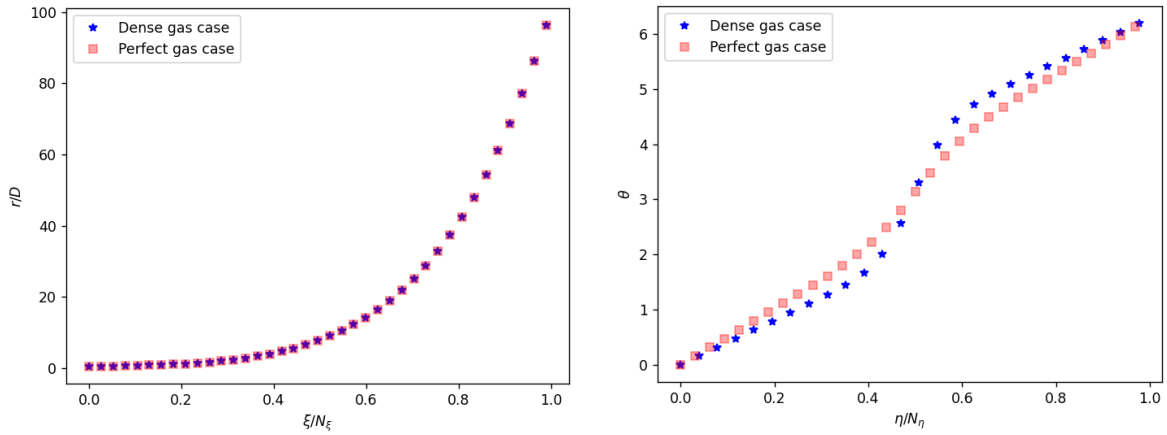

Figure 2. Radial and azimuthal mesh spacing as a function of mapped radial and azimuthal coordinates. In these figures, every tenth mesh point is plotted.

At the wall, an isothermal temperature boundary condition is applied for both the dense gas and perfect gas cases to enable heat transfer. The wall and freestream temperature conditions are informed by our previous study on heat transfer effects in turbulent boundary layer flows [11] and chosen to straddle the critical point and Widom line to capture the steepest gradients in density and thus more variability in heat transfer effects. The thermodynamic properties are modeled using the Peng-Robinson equation of state [12] and the dynamic viscosity and thermal conductivity are computed using transport relations from Chung et al. [13] that consider both temperature and pressure effects.

All simulations were run with an in-house solver, PadeLibs. The simulations solve the fully-compressible Navier-Stokes equations using sixth-order compact-finite-difference schemes. For the perfect gas case, the flux blending threshold was set to 0.8 to damp spurious oscillations, and for the dense gas case, the flux blending threshold was set to 0.9999. Here, the flux blending threshold represents the weight of central schemes used versus first-order

upwind schemes. The simulation domain has a radius of 100 cylinder diameters, and a numerical sponge is applied at a radius of 50 cylinder diameters to regularize flow in the far-field region. In addition, to further damp spurious oscillations in the coarse-mesh region, the numerical scheme is manually set to be first-order upwind at a radius of 25 cylinder diameters.

PRELIMINARY RESULTS AND DISCUSSION

The dense and perfect gas cylinder cases were each run for approximately 100 cylinder-diameter-based-flow-throughs after reaching steady-state flow, and data were sampled frequently to generate the spectra shown in this section. Figure 3 shows instantaneous subgrid-scale (SGS) viscosity contours normalized by total viscosity in the near wake of the cylinder for both dense and perfect gas flows. Near the wall, the SGS viscosity is small compared to the magnitude of the total viscosity thus justifying the quality of the LES.

Figure 4 shows plots of the centerline velocity and pressure coefficient for the perfect and dense gas cases. The angular coordinate for the pressure coefficient is defined such that the front stagnation point corresponds to a value of π/2. The curves in the centerline velocity plot are not completely smooth, though they do not shift greatly with different averaging windows, and the curve for the perfect gas case rises slightly above zero near the wall. This suggests that the simulations could run farther to enhance averaging. The trough of the centerline velocity for the dense gas case appears to be shifted radially outwards from that of the perfect gas case. In addition, the trough for the pressure coefficient appears slightly more diffuse for the dense gas case than the perfect gas case. These trends are consistent with the fact that the dense gas case is much more viscous than the corresponding perfect gas case at the same density ratio. Visually, the SGS contours in Figure 3 also appear slightly more diffuse for the dense gas case than the perfect gas case.

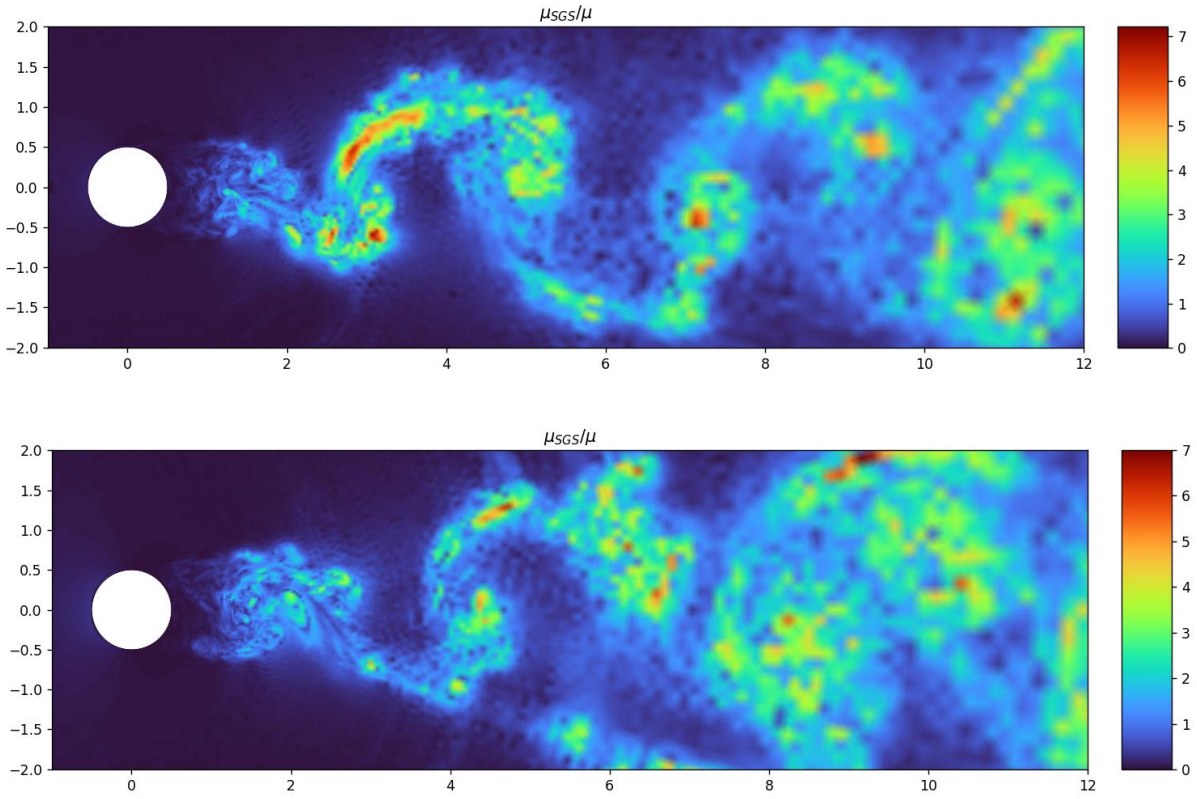

Figure 3. Comparison of SGS viscosity in near wake for perfect gas (top) and dense gas (bottom) cases.

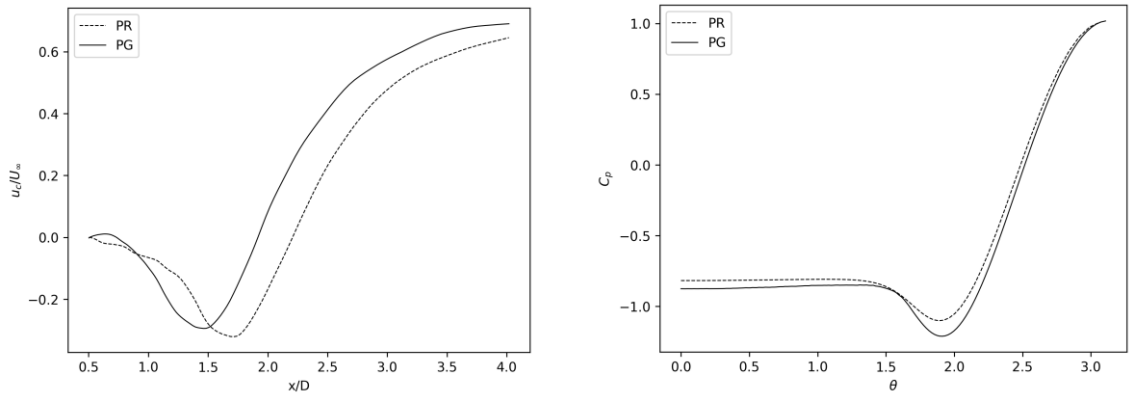

Figure 4. Centerline velocity (left) and pressure coefficient (right) for perfect and dense gas cases.

Figure 5 shows defect profiles of temperature, density, enthalpy, and thermal conductivity taken at a vertical probe located 1.54 cylinder diameters away from the cylinder wall. The probe location follows analysis done by Song et al. (2024) and Kravchenko and Moin (2000) [9, 14]. The perfect gas case appears to incur a more severe temperature deficit than the dense gas case; this makes sense given that the reduced freestream temperature is 1.50 for the perfect gas case but only 1.15 for the dense gas case. For the density, enthalpy, and thermal conductivity deficit profiles, the dense gas case appears to show narrower peaks at vertical locations greater than one cylinder diameter from the centerline and a far greater deficit at vertical locations close to the centerline.

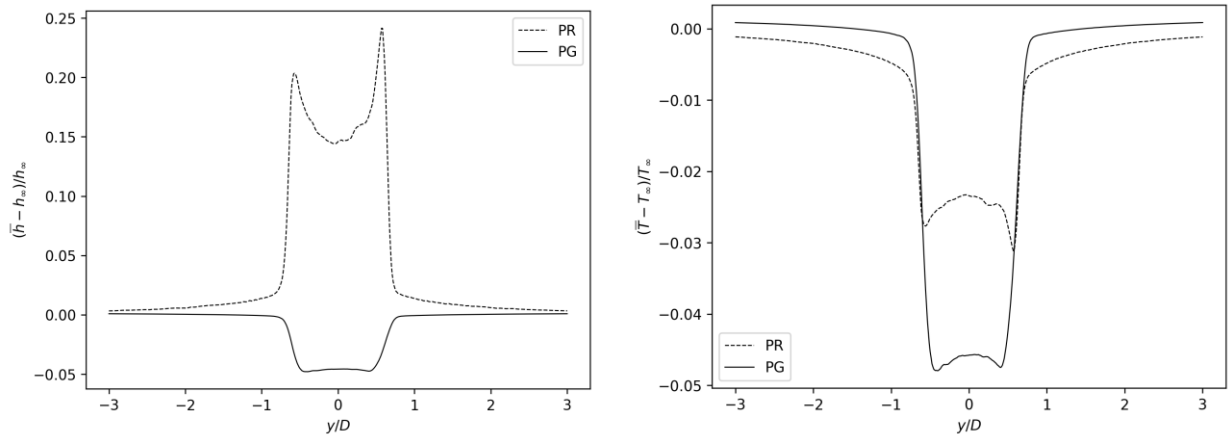

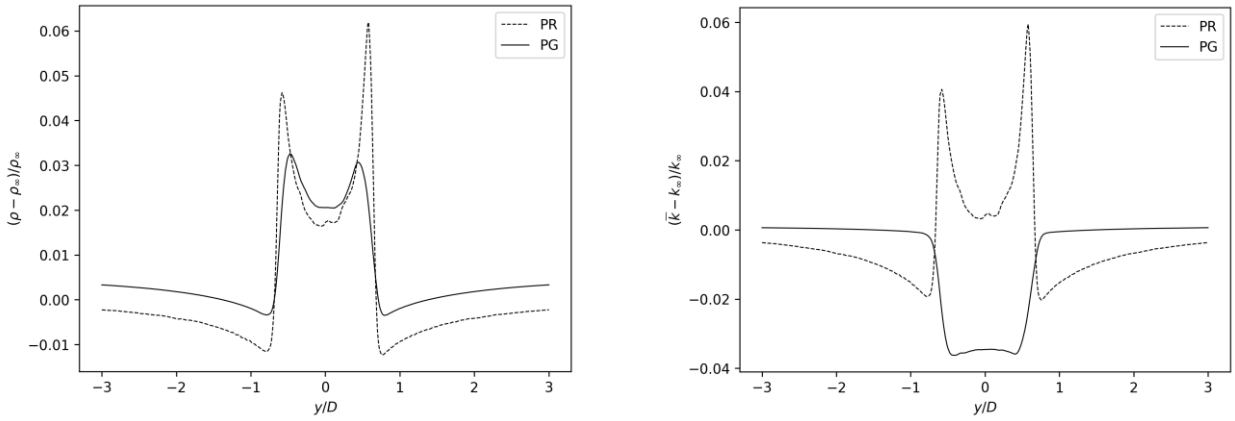

Figure 5. Defect profiles of enthalpy (top left), temperature (top right), density (bottom left) and thermal conductivity (bottom right) taken at a value of x/D of 1.54.

Figure 6 shows power spectral density (PSD) curves for the lift coefficient (C_L), drag coefficient (C_D), and integrated wall heat flux around the cylinder wall (q_w). The PSD for the drag coefficient show a peak at a Strouhal number approximately two times that of the lift coefficient for both dense and ideal gas cases. The C_L peaks occur at Strouhal numbers of 0.672 and 0.649 and the C_D peaks occur at Strouhal numbers of 1.326 and 1.39 for the dense and perfect gas cases respectively. However, there is no significant peak in the PSD of q_w for either case, and the signal is much weaker than that of C_L or C_D. Currently, an SPOD analysis is being carried out to determine the dominant frequencies corresponding to heat transfer in the cylinder flows. Preliminary SPOD results using enthalpy, temperature, and density as signals suggest low Strouhal numbers of approximately 0.2 and 0.4 as corresponding to the dominant eigenvalues. The Strouhal number of 0.2 likely corresponds to the vortex shedding frequency, and the Strouhal number of 0.4 appears to be a strong harmonic of this shedding frequency.

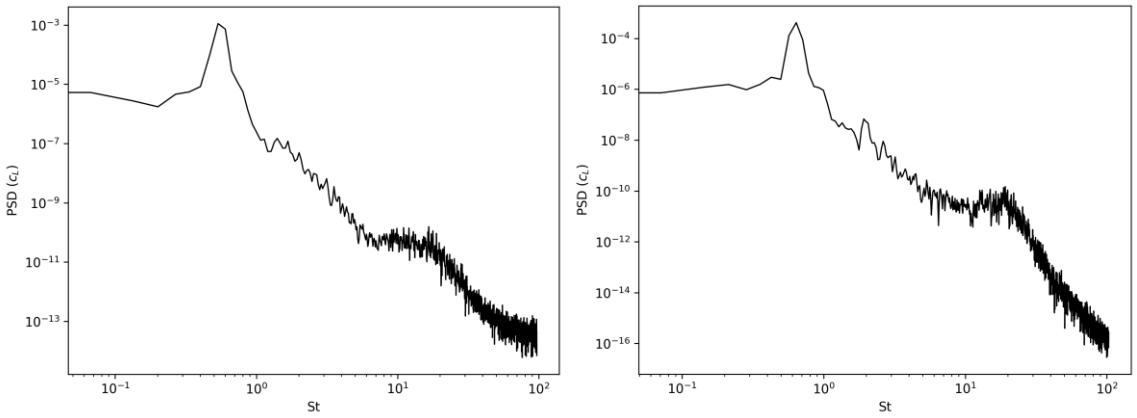

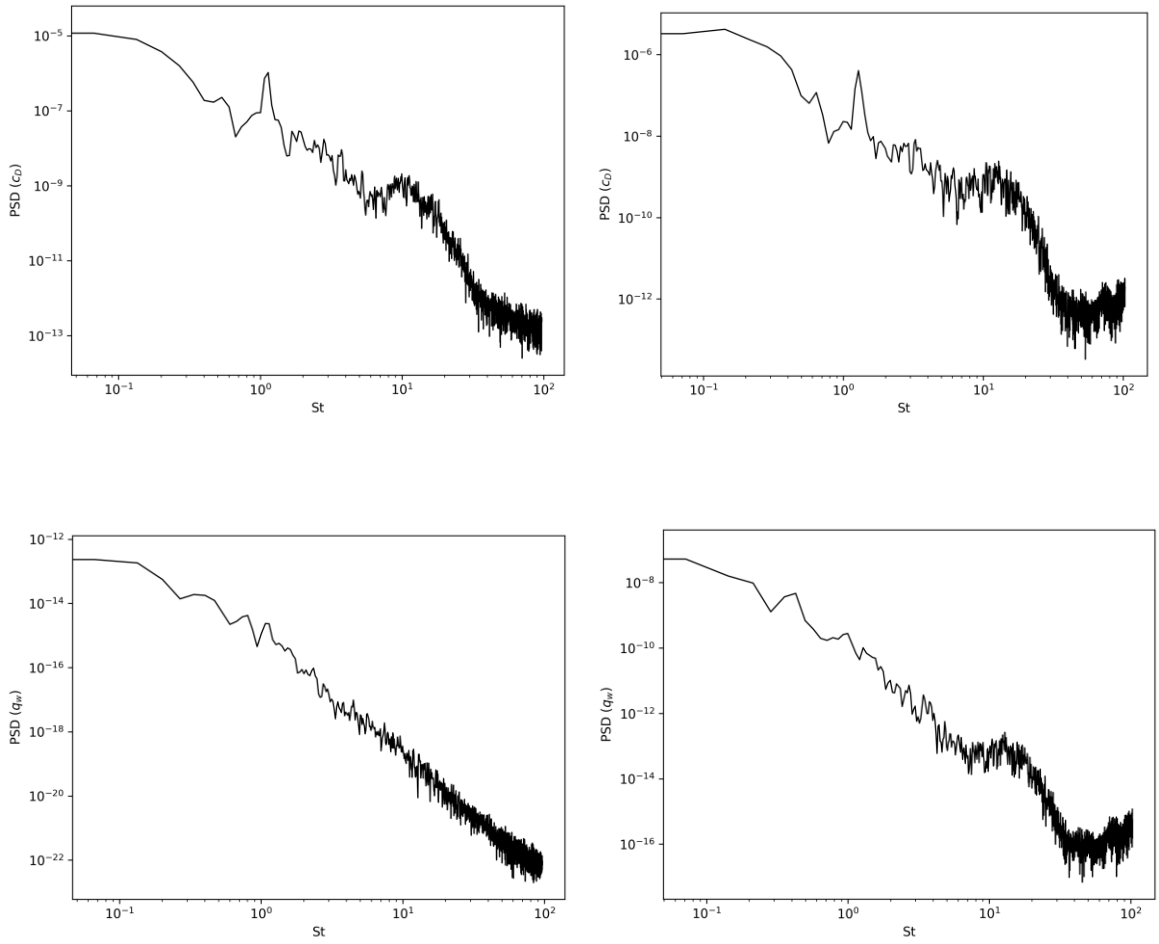

Figure 6. Power spectral density (PSD) curves of the lift and drag coefficients (top row, middle row) and wall heat flux (bottom row). The left column represents the perfect gas case, and the right column represents the dense gas case.

REFERENCES

[1] Abdelghafar, M. M., Hassan, M. A., & Kayed, H. (2025). Direct integration of supercritical carbon dioxide-based concentrated solar power systems and gas power cycles: Advances and outlook. Applied Thermal Engineering, 126064.

[2] Guo, J.-Q., Li, M.-J., He, Y.-L., Jiang, T., Ma, T., Xu, J.-L., and Cao, F., “A systematic review of supercritical carbon dioxide (S-CO2) power cycle for energy industries: Technologies, key issues, and potential prospects,” Energy Conversion and Management, Vol. 258, 2022, p. 115437.

[3] Brun, K., Friedman, P., & Dennis, R. (Eds.). (2017). Fundamentals and applications of supercritical carbon dioxide (sCO2) based power cycles. Woodhead publishing.

[4] Xie, J., & Xie, G. (2022). Vortex dynamics of supercritical carbon dioxide flow past a heated circular cylinder at low Reynolds numbers. Physics of Fluids, 34(1).

[5] Manda, U., Parahovnik, A., Mazumdar, S., & Peles, Y. (2023). Heat transfer characteristics of turbulent flow of supercritical carbon dioxide (sCO2) in a short-heated microchannel. International Journal of Thermal Sciences, 192, 108389.

[6] Gabriel-Ohanu, E., Shah, A., Khadse, A., Fernandez, E., & Kapat, J. S. (2024). Experimental and Numerical Investigation of Effect of Inclination on sCO2 Heat Transfer in a Circular Pipe. ASME Journal of Heat and Mass Transfer, 146(4), 041803.

[7] Gabriel-Ohanu, E., Shah, A., Khadse, A., Fernandez, E., & Kapat, J. S. (2024). Experimental and Numerical Investigation of Effect of Inclination on sCO2 Heat Transfer in a Circular Pipe. ASME Journal of Heat and Mass Transfer, 146(4), 041803.

[8] Bamido, A., Dhir, V. K., Prasad, V., & Banerjee, D. (2020, July). A Numerical Study of Forced Convective Heat Transfer Characteristics of Supercritical Fluid in a Horizontal Circular-Pipe. In Heat Transfer Summer Conference (Vol. 83709, p. V001T11A001). American Society of Mechanical Engineers.

[9] Song, H., Ghate, A. S., Matsuno, K. V., West, J. R., Subramaniam, A., & Lele, S. K. (2024). A robust compact finite difference framework for simulations of compressible turbulent flows. Journal of Computational Physics, 519, 113419.

[10] Song, H., Ghate, A. S., Matsuno, K. V., West, J. R., Subramaniam, A., & Lele, S. K. (2024). A robust compact finite difference framework for simulations of compressible turbulent flows. Journal of Computational Physics, 519, 113419.

[11] Chandra, A., Song, H., & Lele, S. (2025). Heat Transfer Effects in Dense-Gas Turbulent Boundary Layer Flows. In AIAA SCITECH 2025 Forum (p. 2414).

[12] Peng, D. Y., & Robinson, D. B. (1976). A new two-constant equation of state. Industrial & Engineering Chemistry Fundamentals, 15(1), 59-64.

[13] Chung, T. H., Ajlan, M., Lee, L. L., & Starling, K. E. (1988). Generalized multiparameter correlation for nonpolar and polar fluid transport properties. *Industrial & engineering chemistry research*, *27*(4), 671-679.

[14] Kravchenko, A. G., & Moin, P. (2000). Numerical studies of flow over a circular cylinder at Re D= 3900. *Physics of fluids*, *12*(2), 403-417.

ACKNOWLEDGEMENTS

The authors would like to acknowledge computational resources from the Discover ACCESS allocation program and the supercomputer *Bridges-2* at the Pittsburgh Supercomputing Center and research support from NASA grant/cooperative agreement NASA-80NSSC22M0108. H.S. is supported by the Center for Turbulence Research Postdoctoral Fellowship, and A.C. is supported by the TomKat Center for Sustainable Energy Graduate Fellowship for Translational Research.